Journal of Nuclear Materials 389 (2009) 248–253

Contents lists available at ScienceDirect

Journal of Nuclear Materials

journal homepage: www.elsevier.com/locate/jnucmat

Characterization of high energy ion implantation into Ti–6Al–4V

M.P. Carroll [a], K. Stephenson [a,*], K.O. Findley [b]

[a] School of Mechanical and Materials Engineering, Washington State University, P.O. Box 642920, Pullman, WA 99164, USA
[b] Metallurgical and Materials Engineering Department, Colorado School of Mines, 1500 Illinois St., Golden, CO 80401, USA

A B S T R A C T

Ion implantation is a surface modification process that can improve the wear, fatigue, and corrosion resistance for several metals and alloys. Much of the research to date has focused on ion energies less than 1 MeV. With this in mind, Ti–6Al–4V was implanted with Al^{2+}, Au^{3+}, and N^+ ions at energies of 1.5 and 5 MeV and various doses to determine the effects on strengthening of a high energy beam. A post heat treatment on the specimens implanted with Al^{2+} samples was conducted to precipitate Ti_xAl type intermetallics near the surface. Novel techniques, such as nanoindentation, are available now to determine structure-mechanical property relationships in near-surface regions of the implanted samples. Thus, nanoindentation was performed on pre-implanted, as-implanted, and post heat treated samples to detect differences in elastic modulus and hardness at the sub-micron scale. In addition, sliding wear tests were performed to qualitatively determine the changes in wear performance. The effect of this processing was significant for samples implanted with Al^{2+} ions at 1.5 MeV with a dose higher than 1×10^{16} ions/cm^2 where precipitation hardening likely occurs and with N^+ ions.

1. Introduction

Advanced titanium alloys are utilized in a wide variety of applications due to factors such as superior specific modulus and strength, corrosion resistance, and biocompatibility. Ti–6Al–4V is an important nonferrous alloy that has found use in fields ranging from aerospace structures to biomedical implants. Improvements in hardness, wear, and fatigue properties are necessary to optimize performance in these applications. The effects of ion beam modification on the mechanical properties of several metals and alloys has been noted in past research [1,2], which has focused mainly on low energy (~keV) treatments. Results from high energy modification and the results of post-processing remain largely unknown. Additionally, tools such as nanoindentation are currently available to better assess implantation effects that were not available for much of the previous work in this area. This study aims at investigating the changes in mechanical properties when Ti–6Al–4V is implanted with Al^{2+}, Au^{3+}, and N^+ ions at MeV energies and then heat treated (Al ion implantation only) to promote intermetallic precipitation.

Possible strengthening mechanisms due to implantation include solid solution strengthening, secondary phase formation, amorphization, and induced residual stress. The dominant mechanism for a given system is highly dependent on experimental conditions such as target material, ion species, beam energy, and dose. For example, with certain ion-material combinations, amorphization may be induced at the surface of a material, thus inhibiting slip band crack formation during fatigue [3]. This was believed to be a possible strengthening mechanism in the gold ion implanted samples because of their large size and the large number of vacancies they create in a Ti–6Al–4V matrix as predicted by the Stopping Range of Ions in Matter Program (SRIM-2000 and SRIM-2008) [4]. For the nitrogen implanted samples, it was expected that strengthening would be due to solid solution strengthening due to their large size misfit with the matrix material [5]. Another possibility is that N^+ ions form TiN precipitates above some critical dose of ions [6,7].

Recent work [8] found that the Ti_3Al and TiAl phases could be precipitated from commercially pure titanium at keV energies with high doses. This precipitation at the surface is helpful for improving wear resistance, as the phases formed are harder than the bulk. The enhanced microstructure is also more resistant to fatigue crack growth, as it may assist in slip band homogenization where dominant slip band nucleation and growth is significantly hindered. The optimal condition to ensure this requires a uniform dispersion of fine precipitates that remain close to the surface [1]. Substitutional solid solution strengthening is also possible for both the Al^{2+} and Au^{3+} implanted specimens.

The degree of strengthening due to possible solid solution strengthening, surface amorphization, and precipitation is assessed in this investigation using N^+, Au^{3+}, and Al^{2+} ions. The initial hypothesis was that the implantation of N^+ ions would result in solid solution strengthening and precipitation strengthening, the implantation of Al^{2+} ions would mainly produce precipitate or intermetallic strengthening after a prescribed heat treatment,

* Corresponding author.
E-mail address: kstephenson@wsu.edu (K. Stephenson).

0022-3115/$ - see front matter © 2009 Elsevier B.V. All rights reserved.
doi:10.1016/j.jnucmat.2009.02.008

and the implantation of high energy Au^{3+} ions would possibly produce amorphous regions on the surface or solid solution strengthening. The hypothesis was largely supported by experimental mechanical property measurements except for the case of the Au^{3+} ion implantation.

2. Experimental procedures

The Stopping Range of Ion in Matter (SRIM) program [4], a Monte Carlo simulation of ion transport phenomena, was used to predict ion range and collision event distributions for the experimental implantation processes. A program such as this is necessary for predicting post-implantation behavior because it contributes a physical understanding of the process with empirical results that allows proposed mechanisms for modified properties to be identified for high dose implantation [9]. SRIM was also instrumental in determining the effects of varying parameters such as ion energy and angle of incidence to the target material.

With the task of improving the surface wear and hardness, optimal conditions were selected that retained the ions close to the surface, created a broad distribution, and maximized collision events without significantly losing ions due to backscattering. According to the SRIM predictions, the angle of incidence had a large effect on this. An angle of 60° between the beam and the sample surface normal was most accommodating to these considerations, and was chosen for each set of experiments. Implantations were carried out at the William R. Wiley Environmental Molecular Sciences Laboratory at Pacific Northwest National Laboratory, a U.S. Department of Energy facility located in Richland, Washington. A total of five sets of experiments were carried out at room temperature, as outlined in Table 1. The variations between sets involved altering the ion energy, dose, and ion species. One specific comparison to note is the Al^{2+} implantation experiments with 1.5 MeV beam energy. One set was implanted with a dose of 1.5×10^{16} ions/cm^2 and the other set was implanted with a dose of 5×10^{16} ions/cm^2; these will be called the 'low dose' and 'high dose' conditions for comparison throughout the rest of the paper.

Post-implantation annealing was used to precipitate Ti_xAl type intermetallics in the implanted region while retaining the bulk microstructure. Literature review [8] found that this precipitation occurs at temperatures above 665 °C. Since titanium readily oxidizes above 600 °C, treatment was restricted to an inert atmosphere. The samples were heated in a tube furnace to 700 °C for 1 h in an argon atmosphere and furnace cooled.

Nanoindentation was performed under load control for each material and implantation condition using a Hysitron nanoindenter equipped with a diamond Berkovich tip; the indentation depth may exhibit some scatter at each applied load due to material inhomogeneities. Before the indentation experiments, the indenter tip was calibrated to standard specimens such as tungsten and Fe_3Si to obtain the contact area for the tip as a function of depth; this contact area function is used in both the hardness and modulus calculations. It is important to note that although the same indenter was used for all conditions, the indentation experiments were conducted at different times over the course of a year and thus, the indenter tip radius and contact area function changed. The data in the same plots in this figure were taken at the same time, so the indenter tip radius and contact area function are the same for each individual plot, allowing the data in those plots to be compared.

Table 1
Conditions selected for 5 experimental sets.

Set	Ion	Energy (MeV)	Dose (ion/cm^2)	Current (nA)	Temperature (°C)	Angle (°)
1	Al^{2+}	1.5	1×10^{16}	250	25	60
2	Al^{2+}	5	1×10^{16}	250	25	60
3	Al^{2+}	1.5	5×10^{16}	250	25	60
4	N^{+}	1.5	2.5×10^{16}	500	25	60
5	Au^{3+}	5	2.5×10^{16}	500	25	60

Samples from all three conditions were prepared by polishing through 0.05 μ alumina powder or polished with 0.05 μm silica on a vibratory polisher prior to implantation, and the surface was left untouched after implantation was complete. SEM analysis confirmed that the implantation experiments and heat treatment had minimal effect on the surface roughness of each of the samples. In other words, the surface roughness change due to implantation was not large enough to strongly affect the calculated nanoindenter contact areas used for deriving the hardness and modulus values. The elastic modulus and hardness of the samples were monitored and plotted as a function of the hemispherical plastic zone size underneath the indenter tip, as calculated from the indentation contact area using Eq. (1) below. This is valid for materials within a range of strain hardening exponents of which Ti–6Al–4V is considered acceptable.

$$\text{Plastic Zone Size} = 2.3\sqrt{A/\pi}, \tag{1}$$

where A = contact area of indentation.

Sliding wear tests were performed on the pre-implanted and Al^{2+} implanted specimens. The apparatus consisted of a pin on disk setup [10] using a low carbon steel disk. The disk speed was set to 48 rpm, with an applied load of 122.4 g. Vickers hardness indentations were made on the sample faces; the indent diagonals were measured at regular time intervals during the wear tests and related to the amount of material removed using the known 3-dimensional geometry of the indent. This allowed indentation dimensional changes to be correlated with amount of material removed as a function of time. The geometrical relationships of the indent were conserved through the process.

3. Results and discussion

Fig. 1(a) shows the starting microstructure of the Ti–6Al–4V alloy used in these experiments. It consists of large, equiaxed grains of lamellar α and β phases; the bulk microstructure did not change with implantation at scales resolvable with high resolution scanning electron microscopy. The spacing between the lamellae is approximately 0.75–0.8 μm. Fig. 1(b) shows an AFM image of indents in an ion implanted specimen, which is representative of all the implanted specimens. The indenter usually made first contact with the α phase due to its much larger volume fraction but sometimes had initial contact with the β phase. Despite the difference in mechanical properties between these two phases, the plastic zone, which is much larger than the indenter depth, sampled the material uniformly; therefore, all of the results presented reflect the implantation effects on the overall microstructure and not just on individual phases.

The most interesting nanoindentation results were observed for the high dose aluminum implanted samples as well as the nitrogen implanted samples. An improvement in elastic modulus and hardness is observed for the high dose Al^{2+} samples that have been heat treated to produce an intermetallic phase. The indentation results are shown below in Fig. 2.

While there is a small improvement in hardness and modulus for the implanted specimens without heat treatment, the effect of post heat treating is significant. There is a sharp increase of elastic modulus and hardness when the plastic zone depth is approximately 500 nm. The fact that this effect is observed only as the plastic zone penetrates the implanted layer suggests that the

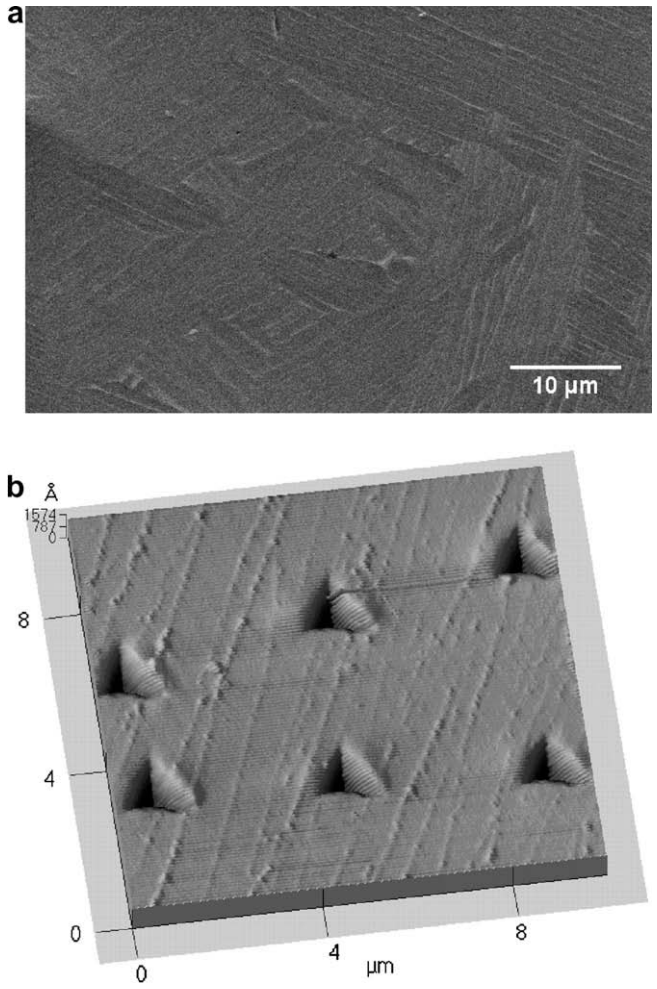

Fig. 1. (a) SEM image of Ti–6Al–4V microstructure of as-received material and (b) AFM image of nanoindents in an implanted microstructure.

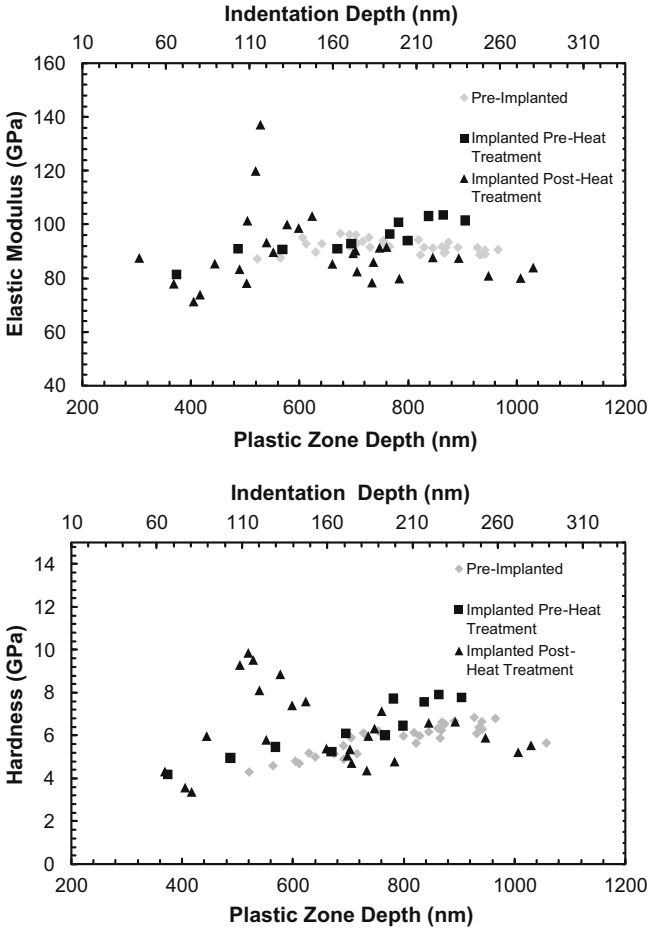

Fig. 2. Elastic modulus and hardness vs. plastic zone depth for the high dose (1.5 MeV, 5×10^{16} ions/cm^2) Al^{2+} implantation experiments.

actual strengthening effect is even more dramatic. Due to these sharp local increases, it may be deduced that a Ti_xAl type intermetallic has been formed, although the exact phase has not been identified. The SRIM predictions for the peaks in the ion projected range appear to be close to the peaks in mechanical properties from the indentation data. Fig. 2 displays peaks around 500 nm, where the SRIM model predicted a peak in the stopping range distribution of 589.5 nm, as shown below in Fig. 3.

Note that there is a small decrease in hardness towards the surface for all of the conditions shown in the figure. Since there is not a corresponding change in modulus, this effect is not due to the contact area calibration. Instead, it is likely due to the self-similarity of the indenter. At small depths, the properties extracted are largely affected by the spherical tip of the Berkovich indenter

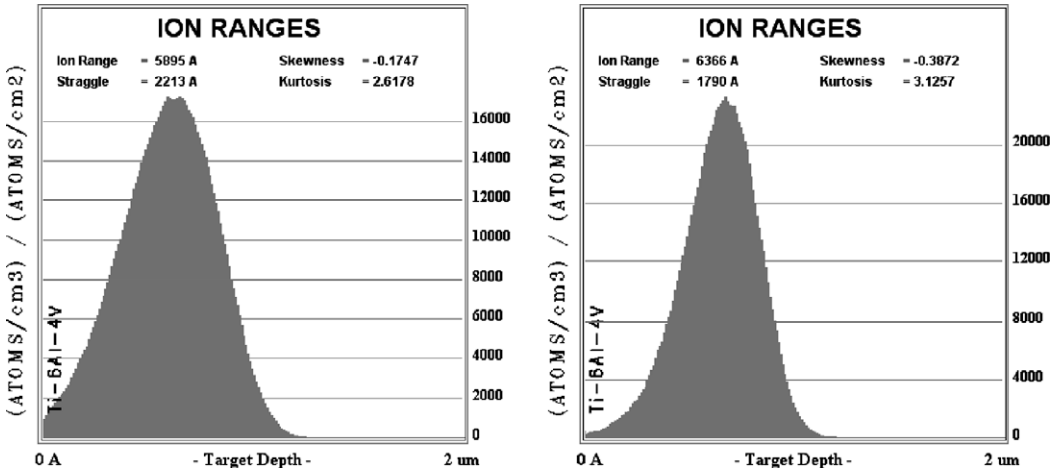

Fig. 3. SRIM predictions of the ion range distributions. On the left, the peak aluminum concentration value occurs at 589.5 nm for the 1.5 MeV Al^{2+} implantations at low and high doses, and 636.6 nm for the N^+ ion implantation on the right.

and the strains induced by the spherical shape are less than those that would be induced by a self-similar Berkovich tip; therefore, the hardness values extracted are low at the small depths, which is solely due to indenter geometry [11]. The radius of the spherical ball at the indenter tip affects the depth at which this occurs and changes over the course of the tip lifetime. Even though the values at the small indent depths are not the true properties of the material, a qualitative comparison between the three conditions can still be made.

A similar but even more definitive effect is shown in the nanoindentation results from the implantations using with N^+ ions (Fig. 4). It is believed that this strengthening effect is due to interstitial solid solution strengthening in the Ti–6Al–4V matrix due to atomic size mismatch [5] and precipitate strengthening due to the formation of TiN precipitates [6,7]. Solid solution strengthening can be attributed to the interaction between dislocations moving on first order prism planes and stationary interstitial solute obstacles, based on the Fleischer–Friedel model [5]. The elastic modulus can also be enhanced in Ti alloys with interstitials, such as N, that increase the charge density between matrix atoms [12]. Fig. 4 demonstrates that the increases in hardness and modulus are substantial. While there may be somewhat of an indentation size effect [13] at the low values of indentation depth that artificially inflate the mechanical property values, a comparison with the pre-implanted and Au^{3+} implanted specimens (Fig. 5) shows that the amount of strengthening due to nitrogen implantation is significant in similar indentation depth ranges. Once again, there is a small decrease in hardness at the surface in Fig. 5 for the same reason that there is the decrease in hardness as explained for Fig. 2.

These results are not unexpected when a comparison is made to implantations using nitrogen ions by Oliver et al. [7]. They performed ion implantations at 90 keV with a current density of 50 mA/m^2 and a dose of 3.5×10^{17} ions/cm^2 and reported a doubling of the base material hardness at a 50 nm indentation depth. Fig. 4 shows that the hardness at 50 nm is also approximately 2× the value of the hardness plateau at large indentation depths despite the difference in implantation conditions. In other words, the increased dose in [7] and the increased energy in this work result in a similar effect at the given indentation depth of 50 nm. A hardness profile is not given in the work by Oliver et al. so the effects of the dose and beam energy differences cannot be compared at the surface or larger depths. For example, we may expect that higher hardness values would be observed in this work at larger depths due to the higher beam energy and larger ion projected range, and a higher hardness is possible in [7] at the surface due to the combination of the lower beam energy and higher dose.

Implanting with Au^{3+} ions does not result in any significant changes in hardness or elastic modulus whatsoever (Fig. 4). Either the amorphous layer formed by the Au^{3+} ions does not increase surface mechanical properties, or the Au^{3+} ion is not an effective substitutional solid solution strengthener in Ti–6Al–4V because the size and modulus mismatch effects for Au in a Ti matrix are negligible. A SRIM simulation with full damage cascades was assessed upon reviewing the data to aid in the interpretation of the results. It was determined that the Au^{3+} ions likely induce a high

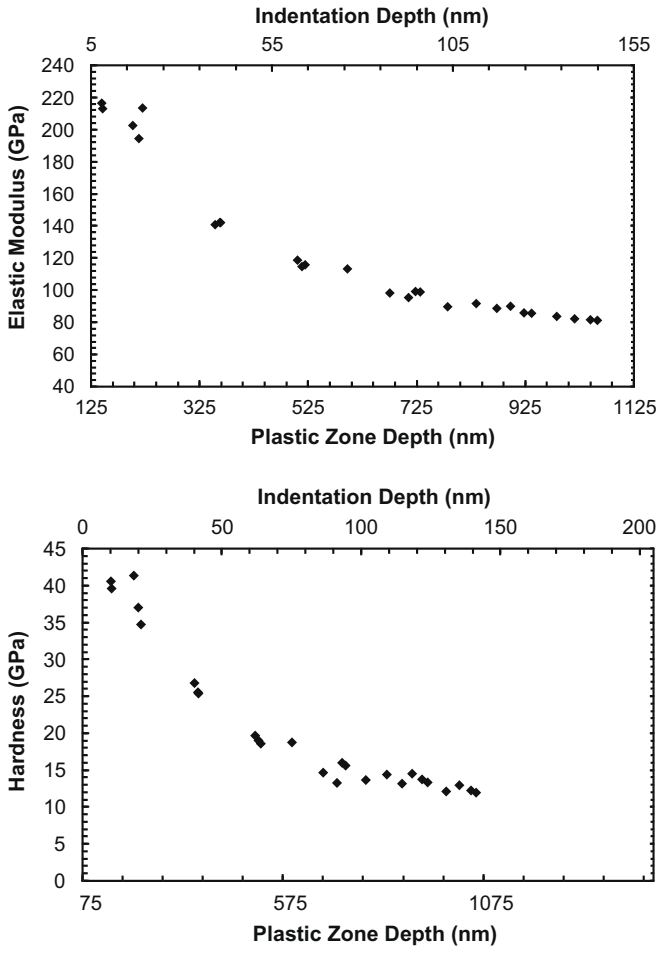

Fig. 4. Elastic modulus and hardness vs. plastic zone depth for the nitrogen implanted specimens.

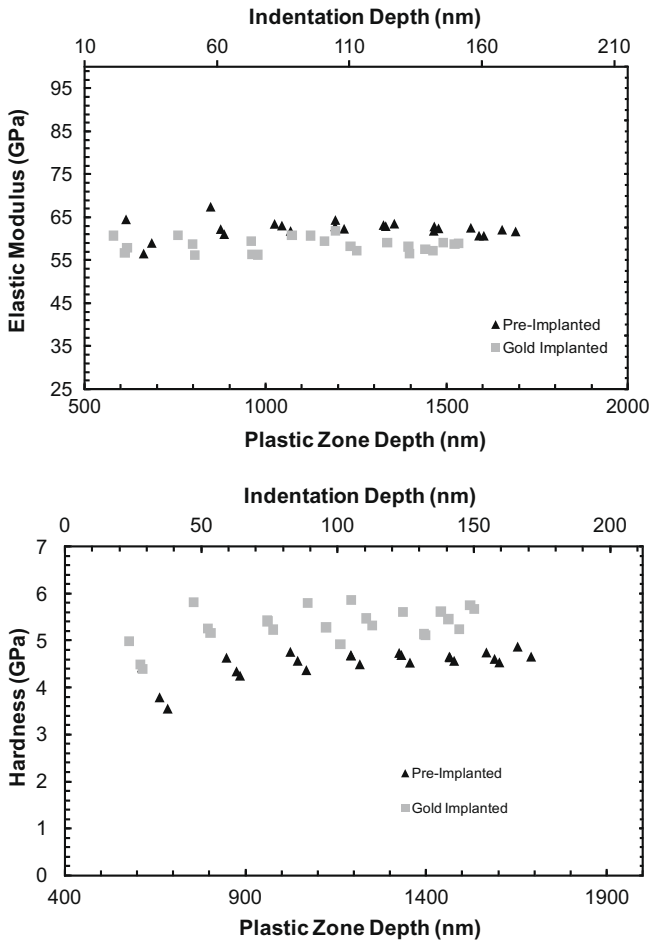

Fig. 5. Elastic modulus and hardness vs. plastic zone depth for the gold implanted specimens.

sputtering yield that causes smooth erosion of the surface throughout the process. A high proportion of nuclear collision cascades as calculated by SRIM also suggest that a small amorphous layer forms. Constant milling of the surface through the process would mean that the final amorphous layer is too thin to measure or offer any practical benefits. The final distribution of ions is determined by the balance of the sputtering rate and the range of implantation of incoming ions. Another noted observation was that the Au^{3+} implanted samples experienced a slight color change at the surface, which supports the hypothesis that the surface had gradually sputtered into previous implantation depths.

The low dose Al^{2+} implanted experimental sets do not display such a large increase in elastic modulus and hardness as the post heat treated condition (Figs. 6 and 7). It is likely that they were not provided with the minimum amount of aluminum to precipitate an intermetallic (~9 wt% for Ti_3Al). This effect is observed for both the 1.5 and 5 MeV beam energies, indicating that the precipitation of the $TiAl_x$ phase is a purely related to accumulating a critical dose of ions. A small increase in hardness and modulus is noted in these experiments for the as-implanted condition, which may be due to solid solution strengthening and lattice distortion. Upon annealing, the elastic modulus and hardness decreases due to possible irradiation enhanced diffusion and vacancy annihilation, but there is relatively little change in hardness. The change in modulus is especially obvious for the specimens implanted with a beam energy of 5 MeV. A large number of vacancies are created for this high beam energy, which makes the effects of irradiation

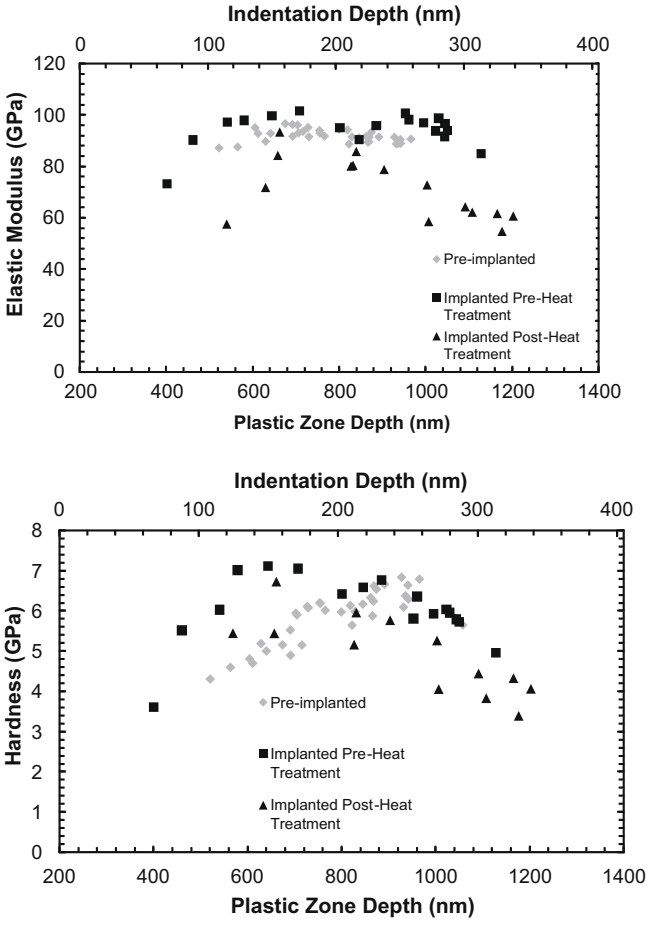

Fig. 6. Elastic modulus and hardness vs. plastic zone depth for the specimens implanted with the lower dose of Al^{2+} (1×10^{16} ions/cm^2) and a beam energy of 1.5 MeV.

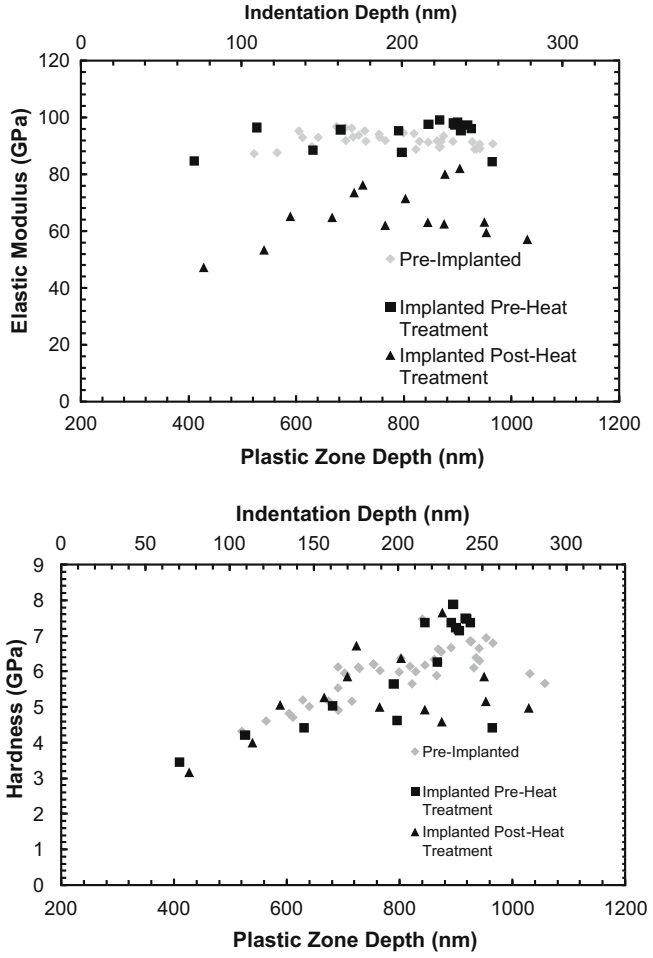

Fig. 7. Elastic modulus and hardness vs. plastic zone depth for the specimens implanted with the lower dose of Al^{2+} (1×10^{16} ions/cm^2) and a beam energy of 5 MeV.

enhanced diffusion prominent upon annealing; the modulus of the post heat treated specimen is significantly lower than the pre-implanted and as-implanted specimens due to probable compositional changes at the surface during annealing. There is very little difference in hardness profiles for the pre-implanted, implanted, and heat treated specimens for this higher beam energy. Again, there is a hardness decrease at the surface that is partially due to the same effect explained for the results in Fig. 2. However, there is also a modulus decrease at the surface, which implies that there was some error in the contact area function at small indenter depths. Nonetheless, even though the values are not the true material properties, they can still be compared because they were obtained with the same indenter.

Vickers hardness measurements were made at depths larger than ion implantation range in the pre-implanted and Al^{2+} implanted specimens before and after heat treatment. The hardness profiles are similar within experimental scatter, showing that the heat treatment did not significantly change the bulk properties and the observed mechanical properties are due to ion implantation effects. Furthermore, the bulk modulus would not change with heat treatment since the modulus is dominated by composition rather than microstructure.

The results from sliding wear tests for the pre-heat treated Al^{2+} are displayed below in Fig. 8. It is evident that the high dose sample shows significant improvement in wear properties near the surface over the pre-implanted sample; since these results are

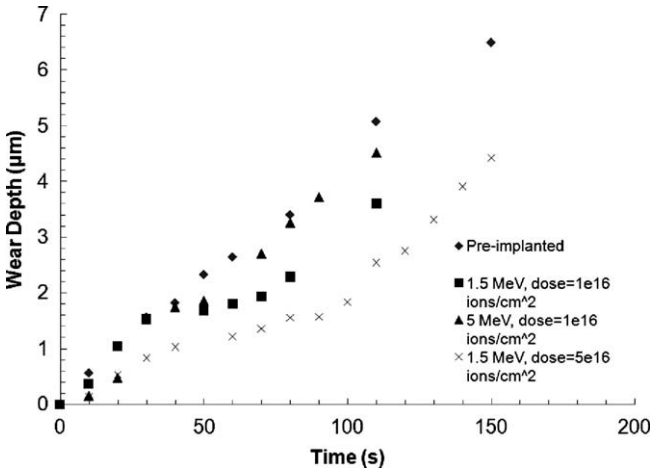

Fig. 8. Thickness of material removed vs. time for pin on disk sliding wear tests performed on the aluminum implanted samples.

for the pre-heat treated specimens, the increased wear resistance is due entirely to solid solution strengthening. The low energy and dose sample also display a lesser improvement. The high energy (5 MeV) samples do not demonstrate a real improvement outside of experimental error because the high energy of the ions results in a significant amount of scatter in the ion distribution and concentration through the sample thickness, which dilutes the solid solution strengthening effect. As samples are worn past their implantation depth (around 2 μm), the wear rates all become parallel, suggesting that the entire implanted region has worn away and the bulk wear resistance of the pre-implanted and implanted specimens is the same.

Accurate sliding wear test data were not obtained for the post heat treated high dose samples because they only exhibited wear in the small regions of the sample that were outside the implantation region; thus, a significant increase in wear resistance was observed but it could not be measured accurately using these sliding wear test methods. Though data is not presented here, it is expected that the specimens implanted with N^+ ions exhibit enhanced wear resistance corresponding to their high surface hardness. Garcia et al. [6] has found that N^+ implantation does substantially improve the wear resistance, though the doses they used are an order of magnitude higher than the ones used here; however, hardness and wear resistance scaled together in their study as it should for these materials. Oliver et al. [7] reported similar increases in wear resistance due to N^+ implantation.

4. Conclusions

Ti–6Al–4V samples were implanted with ions at high energies to determine the changes in mechanical properties. A significant increase in hardness, elastic modulus, and wear resistance was noted for samples treated with Al^{2+} at 1.5 MeV with a dose of 5×10^{16} ions/cm^2 following post process annealing that resulted in the formation of an intermetallic phase on the surface. A significant increase in hardness and modulus was also noted for samples treated with N^+ at 1.5 MeV with a dose of 2.5×10^{16} ions/cm^2. It is believed that these increases were due to interstitial solid solution strengthening with precipitate strengthening also possible. The increase in hardness at the surface from both of these treatments also has potential implications in increasing the fatigue life of Ti–6Al–4V by inhibiting and/or homogenizing slip band crack initiation.

Al^{2+} samples treated at lower doses of 1×10^{16} ions/cm^2 and a beam energy of 1.5 MeV showed moderate increases due to solid solution strengthening, but did not experience improvements from annealing since the critical aluminum concentration for intermetallic formation was not provided. The surface mechanical properties were not improved significantly using Au^{3+} implantation; any possible amorphous layer produced during implantation was likely removed by sputtering and the effects of Au ion solid solution strengthening are small. Thus, the ion beam parameters would have to be revised to achieve any increase in the surface mechanical properties using Au^{3+} ions to avoid the detrimental sputtering effect.

Acknowledgements

The authors wish to acknowledge the contributions of several parties including the EMSL User Facility at Pacific Northwest National Laboratories, specifically, Vaithiyalingam Shutthanandan who helped carry out the ion implantation experiments. We also wish to thank Stefhanni Jennerjohn and Professor David Bahr for their help in conducting and analyzing the nanoindentation data. Finally, this work was supported through the National Science Foundation: Division of Materials Research REU site program under Grant No. 0453554.

References

[1] R.G. Vardiman, The Modification of Fatigue Properties by Ion Implantation, Ion Plating and Implantation Applications to Materials, ASM, 1986. p. 107.
[2] J.M. Williams, R.A. Buchanan, E.D. Rigney Jr., Improvement in Wear Performance of Surgical Ti–6Al–4V Alloy by Ion Implantation of Carbon or Nitrogen, Ion plating and Implantation Applications to Materials, ASM, 1986. p. 141.
[3] H. Pelletier, D. Muller, P. Mille, J.J. Grob, Surf. Coat. Technol. 158&159 (2002) 301.
[4] James F, Ziegler. Particle Interactions with Matter. <http://www.srim.org/>, 2008.
[5] E. Collings, H. Gegel, Physics of Solid Solution Strengthening, Metallurgical Society of AIME, AIME, 1973. p. 1.
[6] J.A. Garcia, A. Guette, A. Medrano, C. Labrugere, M. Rico, M. Lahaya, R. Sanchez, A. Martinez, R.J. Rodriguez, Vacuum 64 (3&4) (2002) 343.
[7] W.C. Oliver, R. Hutchings, J.B. Pethica, The Wear Behavior of Nitrogen-Implanted Metals, Metallurgical Transactions A vol. 85A, 1984, p. 2.
[8] I. Tsyganov, E. Wieser, W. Matz, A. Mucklich, H. Reuther, Nucl. Instrum. Methods 161–163 (2000) 1069.
[9] E.W. Thomas, The Physics of Ion Implantation, Ion Plating and Implantation Application to Materials, ASM, 1986. p. 7.
[10] Hawk, JA, Abrasive Wear Testing, ASM Handbook, vol. 12, Mechanical Testing and Evaluation, ASM International, 2000, in ASM Handbooks Online, <http://www.asmmaterials.info> ASM International, 2000.
[11] D. Tabor, The Hardness of Metals, Oxford University, 1951.
[12] Y. Song, Z.X. Guo, Philos. Mag. A 82 (7) (2002) 1345.
[13] J.G. Swadener, E.P. George, G.M. Pharr, J. Mech. Phys. Solids 50 (4) (2002) 681.